Design and Testing of Off Axis Illumination Filters for a 248nm DUV Exposure System

Matthew E. Malloy

Abstract—**This study involves the design and testing of off axis illumination apertures for an ASML 5500/90 248nm DUV stepper. X and Y slot pole apertures based on dipole theory were designed, fabricated out of aluminum, and inserted into the optical column of the stepper. Test patterns consisting of vertically oriented features were printed with and without dipole illumination, exposed, and compared to determine their effectiveness. As expected, features which were to small to print under standard illumination imaged exceptionally well using the x slot pole aperture. The y slot pole aperture delivered the same results as standard illumination which was also expected. 0.24μm features were printed clearly and consistently under the off axis illumination scheme on a system specified to print a minimum feature size of 0.35μm with a numerical aperture of 0.5.**

Index Terms— **off axis illumination; dipole; slot pole; aperture design**

I. Introduction

There are quite a few options available to the lithography engineer when designing a new process; some more feasible than others. These options include new equipment and tools, reticle enhancement techniques such as phase shifting masks and optimal proximity correction, and off axis illumination (OAI) to name a few. While the purchase of a high NA and low wavelength imaging system may guarantee results, it may not be the most cost effective method of doing so. A great deal of effort has been applied towards improving the capability of current lithography processes without such an investment. Optical lithography is being pushed to its limits in terms of NA, sigma, and wavelength, and all of the aforementioned techniques are being used to extend and perfect current systems. Of the various methods currently applied, off axis illumination is one of the most easily implemented and cost efficient ways to increase both resolution and depth of focus. Unlike standard illumination where diffraction energy required to image is pushed beyond the limits of the projections lens, off axis techniques adjust the angular distribution to improve image capture capability. Depth of focus is also increased due to overlap of the 0^{th} and $\pm 1^{st}$ diffraction orders. Dipole, quadrupole, and annular are just a few of the many types of off axis illumination used today.

Lithographic imaging systems are most accurately described by a few key parameters including the illumination wavelength (λ), method of illumination, numerical aperture (NA), and partial coherence (σ). These are the main tools lithography engineers have to work with when developing and optimizing new processes. By utilizing off axis illumination one should be able to push the resolution limits of a given imaging system far past what it was originally designed to print. Also, the DOF is increased. The DOF is, "the range of focus errors that a process can tolerate and still give acceptable lithographic results," as stated by Chris Mack [1]. These parameters will be defined by presenting a typical lithography system, followed by a theoretical and practical discussion on the implementation of dipole and slot pole illumination schemes.

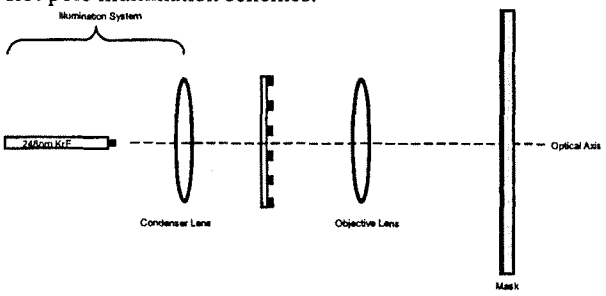

Fig. 1. General illustration of typical lithographic projection system such as that used in the 5500/90 ASML stepper.

Matt E. Malloy is an undergraduate Microelectronic Engineering student at the Rochester Institute of Technology, Rochester, NY 14623 USA (Phone number: 585-739-4536; e-mail: mem2271@rit.edu).

The most important part of any illumination system is the source as there would be no imaging without one. In this case, the source is a Krypton Fluoride (KrF) laser at a deep ultra violet wavelength of 248nm. Laser sources are capable of producing nearly coherent illumination; that is, they can be treated almost as point sources. Next, there is the condenser lens which is responsible for diffusing the energy provided by the source to ensure that the mask is illuminated with a uniform distribution of light. As labeled in the diagram, the condenser lens along with the light source make up the illumination system. The third component shown in Figure 1 is the mask containing the image which will be reduced four or five times and projected towards the wafer by the objective lens. The objective lens handles the increasingly difficult task of collecting as much information as possible in order to create an image that closely resembles the original design.

A reasonable amount of geometric optics theory is required to fully understand the functioning of a system like this. Fortunately, the main ideas are quite simple to explain. To start, one should know that that the configuration depicted in Figure 1 is based on Köhler illumination where an image of the source, by means of the condenser, is created at the entrance pupil of the objective lens [2]. This image is then projected towards the wafer where it should come into focus in the resist. In the case of the ASML stepper system used for this project, an integrator, or "fly's eye" lens is inserted before the condenser which helps to control the light intensity and uniformity entering the optical column. The integrator lens becomes the source that is "seen" at the objective lens. Figure 2(a) shows the integrator lens and 2(b) shows how its image is projected by the illumination system towards the wafer.

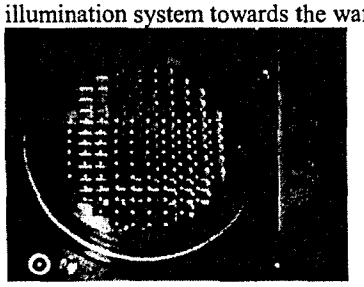

Fly's Eye Lens and its image

Fig. 2. (a) Picture of fly's eye lens from an ASML 5500/90 DUV stepper and (b) it's image as projected towards the wafer.

Now that the basics of this Köhler illumination system have been described it is possible to discuss how features on the mask are imaged in the resist. Diffraction theory will be the basis of this discussion. When light passes through a diffraction grating (or a series of lines and spaces on a photomask), it appears to bend as it spreads out in all directions. The resulting diffraction pattern creates an electric field distribution which under standard illumination conditions produces bright fringes along the optical axis (OA). These bright fringes are in increments of plus and minus λ/p where λ is the wavelength of the system and p is the combination of one line and its adjacent space, otherwise known as the pitch. Figure 3 illustrates this situation for a theoretical point source on the optical axis. In order for image modulation to occur, a minimum of the 0^{th} and some $\pm 1^{st}$ diffraction order information must be collected by the objective lens. The 0^{th} order provides intensity but no feature information, while the higher orders provide the pitch information required for modulation. The numerical aperture (NA) which is a function of both the objective lens diameter and its distance from the mask places limits on the amount of information collected. NA is calculated as shown in Figure 4 as the refractive index of the surrounding medium times the sine of the maximum angle at which diffracted information can be captured by the objective.

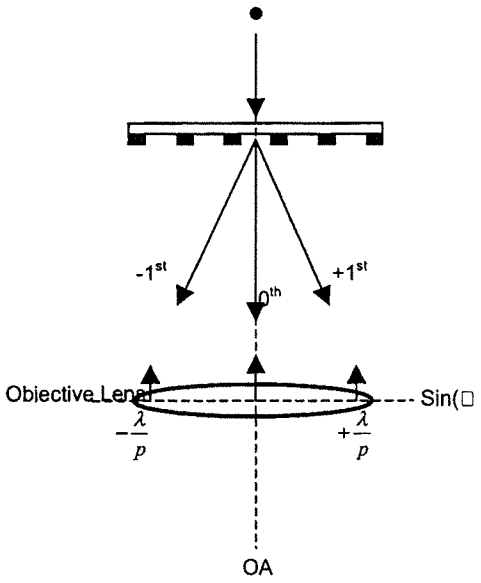

Point source illumination

Fig. 3. Point source illumination of a series of lines and spaces under standard illumination conditions.

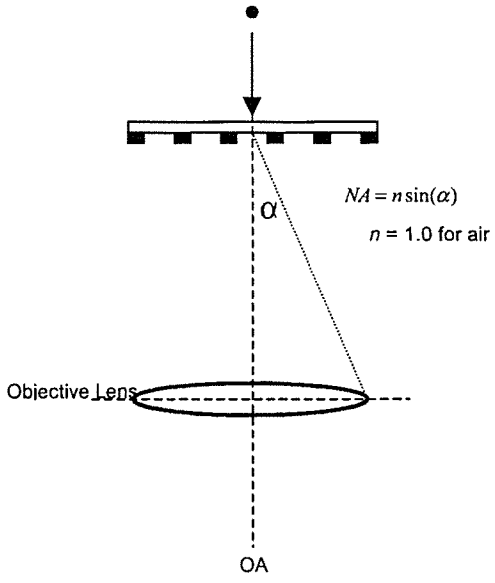

Determining NA

Fig. 4. Shows how the numerical aperture is determined for an imaging system.

The refractive index is usually ignored as it equals one for air. It would take an infinitely large lens capable of collecting all of the diffraction order information in order to create an exact replica of a feature, which at an angle of 90° corresponds to a maximum NA of 1.0. The numerical aperture of the system at hand is 0.5 but may be lowered to 0.4. This means that the maximum angle at which information is collected by the lens with the current setup is 30° on each side of the optical axis.

Knowledge of the source wavelength and NA can be used to determine the minimum theoretical resolution

assuming all other aspects of the tool are optimized and functioning properly. This is shown in Equation 1.

$$R = \frac{0.5\lambda}{NA} \qquad (1)$$

This has been the traditional approach to lithography for the semiconductor industry; but what happens as feature sizes shrink below what can traditionally be imaged? As line sizes decrease, the diffraction orders spread out further and reach a point where the objective lens is only able to capture information from the 0^{th} order. At this point image modulation ceases and the lithography system is termed diffraction limited since diffraction is the main factor controlling the minimum resolvable feature size.. Figure 5 shows the situation where the $\pm 1^{st}$ diffraction orders fall just outside the lens NA.

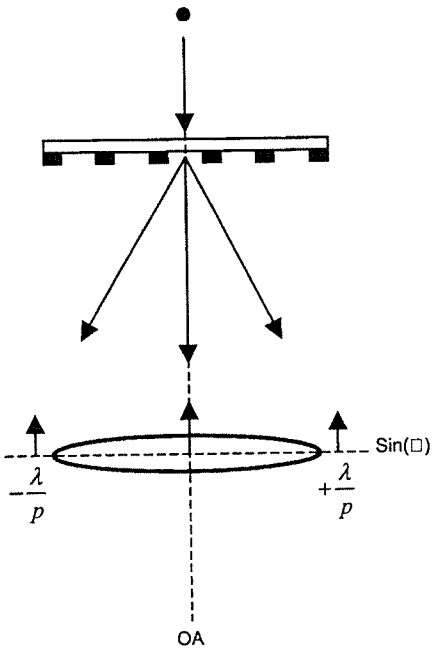

Diffraction Limited Lithography

Fig. 5. This figure illustrates what happens when small feature sizes cause the diffraction orders to spread beyond what the objective lens can capture. Notice how the $\pm 1^{st}$ orders fall just outside the physical limits of the lens.

Up to this point only coherent illumination has been considered; that is, only one point source along the optical axis has been discussed. If this point source is shifted slightly to an off axis location such as that shown in Figure 6 the resulting diffraction pattern shifts as a result.

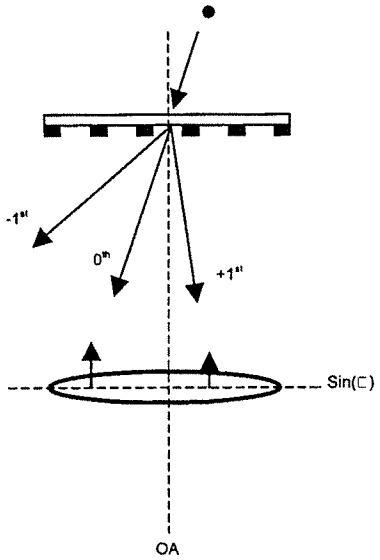

Fig. 6. In this situation the point source has been moved slightly off axis causing the resulting diffraction pattern to shift as well. Now, the objective lens is able to capture information from at least one of the 1st diffraction orders.

The objective lens is now able to collect information from the 0th order and enough first diffraction order information for a limited amount of image modulation. If this idea is extended to a series of point sources, or a single source with a finite width, then each of the resulting diffraction orders will be spread over a finite area as illustrated in Figure 7. The illumination is no longer coherent, but rather partially coherent.

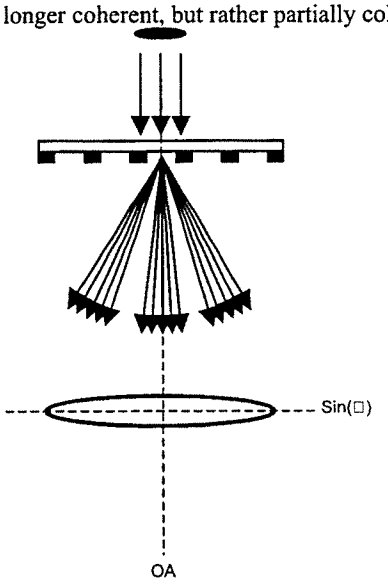

Fig. 7. In this situation, a point source is no longer being used, but it has been replaced with a source of a finite diameter.

If the level of partial coherence were to be increased to the point where the source was the same size as its image, then the system would be using incoherent illumination.

It should be clear from Figure 7 that partial coherence allows us to resolve features that would be impossible with coherent illumination. The degree of partial coherence, designated by σ, also ranges from 0 to 1.0 and is calculated as shown in Equation 2.

$$\sigma = \frac{NAc}{NAo} \qquad (2)$$

where NAc is the numerical aperture of the condenser lens and NAo is the numerical aperture of the objective lens. Partially coherent illumination is only used if the objective lens is unable to capture at least the ±1st diffraction orders produced by coherent illumination. At high levels of partial coherence the interference pattern averaging effects cause severe loss of image modulation. For that reason, incoherent illumination is not used and the level of partial coherence may only approach, but not equal 1.0. For the ASML 5500/90, the fly's eye lens is used to adjust the level of partial coherence by blocking off specific integrator elements with pre-defined apertures. The more elements blocked off, the lower the coherence value is. The partial coherence can be adjusted from 0.3 when blocking all but 36 of the 112 integrator elements to 0.51 with no aperture in place. Pictures of the four sigma limiting apertures are shown in Figure 8.

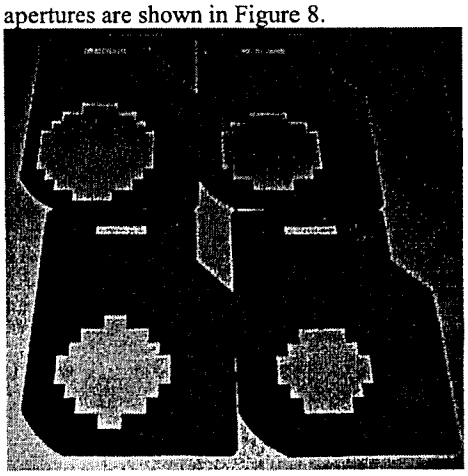

Fig. 8. This is a picture of the four apertures used to adjust the level of partial coherence on an ASML 5500/90 DUV stepper. They are inserted just prior to the fly's eye lens shown in Figure 2.

Off axis illumination is the next logical step when studying the ideas of partial coherence for the purpose of increased resolution capabilities. Off axis schemes are designed for specific pitch and line sizes and like the previous situations, are also based on wavelength and lens NA. The slot pole apertures designed and tested for this project were based on a more traditional design known as dipole illumination. Dipole illumination

schemes will be described first followed by a discussion on the benefits of moving to a slot pole design.

As shown previously, when the source is shifted to an off axis location, the resulting diffraction orders are also shifted making it possible to print features smaller than the limit determined by Equation 1. It has been shown that

$$R = \frac{0.25\lambda}{NA} \qquad (3)$$

is possible with a properly optimized imaging system utilizing dipole illumination [3]. If designed such that the 0^{th} and 1^{st} diffraction orders overlap on each side of the optical axis than an increase in depth of focus will also be realized. In theory, the resulting depth of focus should be infinite since there is no optical path difference between these orders as there was in the previous situations. This of course, assumes zero or very narrow pole width and near zero intensity at the wafer level [4]. Figure 9 depicts this situation.

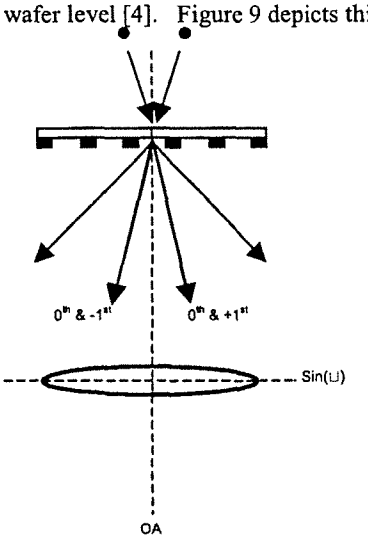

Dipole Illumination

Fig. 9. Dipole illumination scheme where the 0^{th} and 1^{st} diffraction orders overlap to improve both resolution and depth of focus.

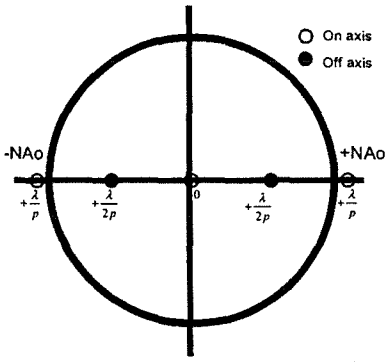

Optical Axis from the Wafer's Point of View

Fig. 10. This is what the wafer "sees" for each type of illumination as it looks up the optical axis

The graphic in Figure 10(a) shows what on axis and dipole illumination looks like if one were to look up at the optical axis from the wafer's point of view. Notice the difference in diffraction orders between the two. Dipole illumination is capable of image modulation where the standard method is clearly unable to image. We see that under standard illumination, the $\pm 1^{st}$ orders fall at $\pm\lambda/p$ which is just outside of the lens NA. The resulting diffraction orders from dipole illumination, on the other hand, fall well within the limits of the objective lens at $\pm\lambda/2p$.

The level of partial coherence has a profound effect on this situation as well; although in a slightly different manner. Whereas the value of σ was increased for standard illumination in an attempt to resolve smaller features, it is increased in this situation in order to accommodate a predetermined range of pitches and feature sizes. For example, Figure 11 shows where the diffraction orders would fall for two distinct pitches.

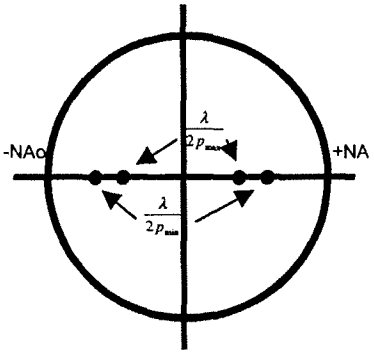

Diffraction orders as a function of pitch

Fig. 11. It is shown here how the pitch determines where a diffraction order falls under dipole illumination. The larger the pitch, the closer the diffraction order falls to the optical axis.

Notice that as the pitch increases, signifying more isolated features, the resulting diffraction order moves closer to the optical axis. On the other hand, dense features cause the diffraction orders to move away from the optical axis.

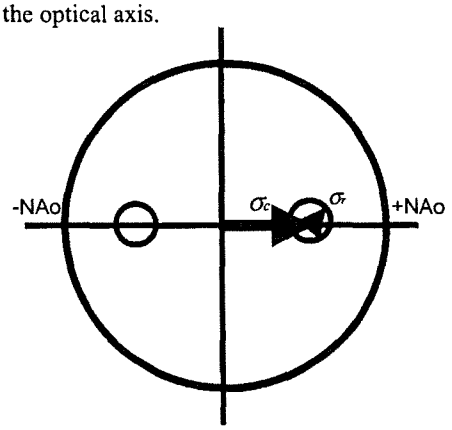

Range of pitch values

Fig. 12. This image shows the range of pitch values determined by the minimum and maximum pitch.

Unlike standard illumination, there are two σ values used to describe this situation. These are: the center sigma, which gives the distance between the optical axis and the center of the poles, and the radial sigma which gives the radius of each pole. If the maximum and minimum pitches are known as shown in Figure 11, than the center σ and radius σ can easily be calculated as shown in the following equations.

$$\text{Center } \sigma: \quad \sigma_c = \frac{\sigma_{c\max} + \sigma_{c\min}}{2} \tag{4}$$

$$\text{where} \quad \sigma_{c\max} = \frac{\lambda}{2p_{\min}NAo} \tag{5}$$

$$\text{and} \quad \sigma_{c\min} = \frac{\lambda}{2p_{\max}NAo} \tag{6}$$

$$\text{Radius } \sigma: \quad \sigma_r = \frac{\sigma_{c\max} - \sigma_{c\min}}{2} \tag{7}$$

If the sigma values are already known than the minimum pitch (corresponding to the densest features) can be determined as follows:

$$p_{\min} = \frac{\lambda}{2NAo(\sigma_c + \sigma_r)} \tag{8}$$

Increasing the range results in larger poles and serves to allow more light, and therefore more intensity, to reach the wafer.

Unfortunately, there are a couple drawbacks to this type of illumination scheme. First, large and isolated feature performance may be sacrificed for the benefit of printing dense features. Second, dipole illumination is only able to accurately image features in one direction. For instance, in the previous few illustrations we see there are poles along the x axis allowing the imaging of vertically oriented features. There are, however, no poles along the y-axis to allow the imaging of horizontally oriented features. Luckily, there are several ways to deal with and overcome this setback. Since dipole illumination is capable of providing excellent benefits some have moved to a two mask process where one mask is created for each orientation. Lithography processes using this system obviously require excellent overlay capabilities. Other off axis techniques like quadrupole and annular illumination may also be used although neither is capable of the resolution enhancements or depth of focus improvements that a dipole configuration can provide. A slot pole design as shown in the following picture provides the benefits of dipole illumination with the added benefit of a small amount of image modulation for features oriented in the perpendicular direction. More importantly, slot poles allow an averaging effect over the height of each pole which functions to supply more light and reduce the effects of lens aberrations. Slot pole apertures are not much more difficult to design than dipoles as the same equations are used for the center and radial sigma. The height of each slot is dependant on the process at hand and must be set so that it does not negatively affect the imaging of the features that the filter was originally designed to print.

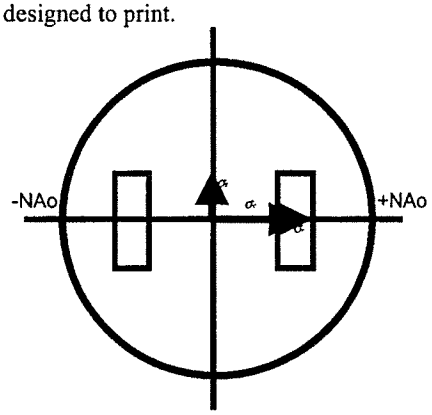

Fig. 12. Slot pole configuration based on a dipole design

As with increasing the size of a dipole, slot poles allow more light to pass resulting in greater intensity at the resist level.

When properly implemented, the above off axis illumination techniques push the limits of optical lithography and they do so with very little cost when compared to the capital required to purchase new equipment. In describing the widespread industry adoption of off axis techniques, Kurt Ronse and Luc Van Den Hove, authors of the paper, *Resolution Enhancement Techniques in Optical Lithography* state that, "Nowadays all advanced steppers are equipped with illuminators allowing one or more types of off-axis illumination. Due to the low added cost, this resolution enhancement technique is definitely the most widespread used in the industry," [5].

II. Experimental Procedure

Prior to beginning this project an in-depth understanding of both on and off axis illumination needed to be achieved. This information was provided via lecture notes and various papers and publications. Second, a thorough understanding of the ASML stepper was required, including knowledge of operating procedures as well as instructions regarding access to the optical column for aperture insertion. It was found that the optical column was easily accessible via a removable panel and UV shield on one side of the tool.

Since the ASML stepper has not yet been qualified and no standard process defined, a great deal of time

was put into determining optimal conditions. This included proper resist handling techniques, optimal coating practices, determining the best focus and exposure, and the creation of a post exposure bake (PEB) and develops process. Characterization began with Arch 8250 DUV resist but was quickly moved to Shipley UV III when it was found that the Arch resist was well past its expiration date and was giving inconsistent results. Uniformity and Focus/Exposure matrices were run using standard illumination to determine the optimal conditions. Standard conditions for this tool include a numerical aperture of 0.5 and partial coherence of 0.51. The NA can be varied from 0.4 to 0.5 but was left at 0.5 for this experiment. It was determined that the optimal exposure for approximately 5750Å of resist was 19mJ/cm^2 with a focus offset of 0μm.

Once it was determined how to access the optical column of the stepper and the original coherence blades were obtained, the design process began. As mentioned previously, these blades as seen in Figure 8 were inserted in front of the integrator lens in order to decrease the level of partial coherence. Figure 13 shows the level of partial coherence for each blade for several NA settings.

Number of Elements \ NA	0.40	0.42	0.44	0.46	0.48	0.50
112	0.64	0.61	0.58	0.55	0.53	0.51 (No blades)
92	0.59	0.56	0.53	0.51	0.49	0.47
64	0.49	0.46	0.44	0.42	0.41	0.39
52	0.45	0.43	0.41	0.39	0.38	0.36
36	0.38	0.36	0.34	0.33	0.31	0.30

Partial Coherence

Fig. 13. Partial coherence as a function of NA and aperture

Physical measurements were made of the integrator lens as shown below and used in combination with the provided blades to design the off axis apertures. Initially, dipole filters were to be created, but once it was determined that each element of the integrator lens was a small rectangle rather than a square, and that the system already had quite a small value of σ, it was decided that slot poles would be more appropriate. A diagram showing the dimensions of the integrator lens and its elements is shown below.

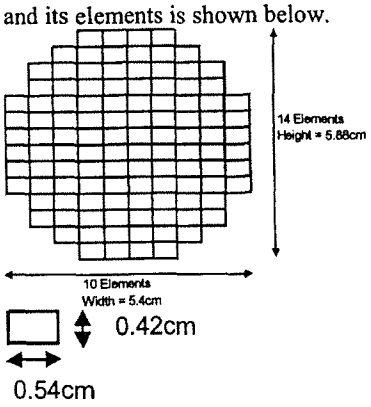

Physical Dimension of Integrator Lens

Fig. 14. This illustration shows the physical dimensions of the entire integrator lens including the dimensions of each element.

Typically, a range of desired pitches would be determined as explained in the theory section of this paper, but since we were starting with a relatively low partial coherence and this work was mainly for educational purposes, we decided to work backwards. That is, slot poles were designed that were pushed almost to the limits of the integrator lens and the resulting pitch range was calculated from there. Figure 15 shows the location of the X and Y poles relative to the fly's eye lens followed by pictures of the actual apertures.

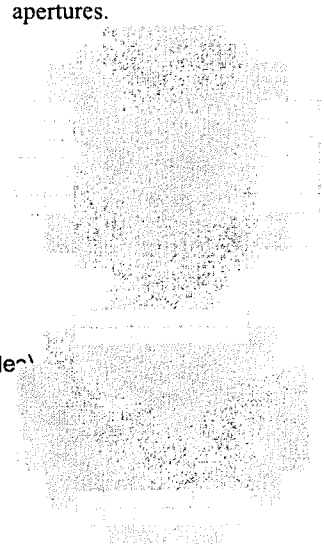

X-slot pole **Y-slot pole**

Fig. 14. Representations of x and y slot poles. The gray areas are those that were blocked off by each aperture while light was allowed to pass in the white areas.

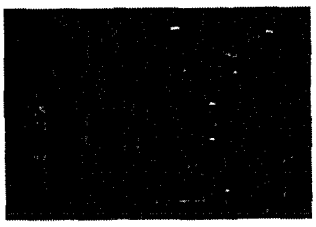

X-slot pole aperture **Y-slot pole aperture**

Fig. 15. Pictures of actual apertures fabricated for this project. These apertures were fabricated in the Mechanical Engineering machine shop at RIT.

The ends of each slot were rounded due to machine shop constraints, but were sufficient for this purpose and each set of slot poles left 24 out of 112 integrator elements open. Once created, the physical dimensions of each aperture were normalized and the corresponding σ's were determined as will be demonstrated next.

First, the physical dimensions of each aperture were measured.

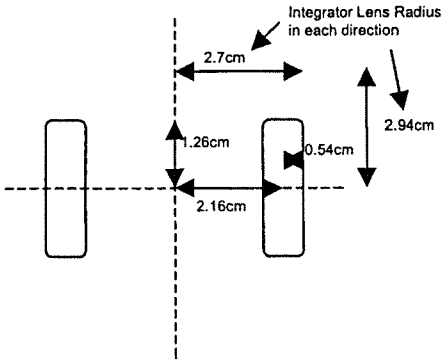

X-slot pole physical dimensions

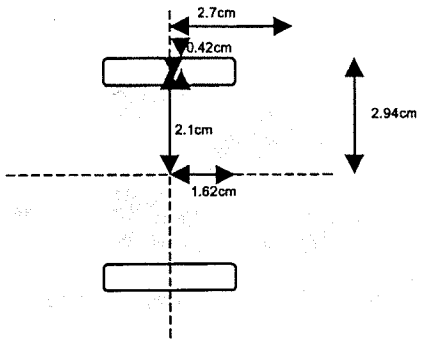

Y-slot pole physical dimensions

Fig. 16. Physical dimension for each aperture

Second, all of the dimensions were normalized to the integrator lens radius in the appropriate direction. Note again that the height and width of this lens are not the equal. The normalized dimensions are shown in Figure 16.

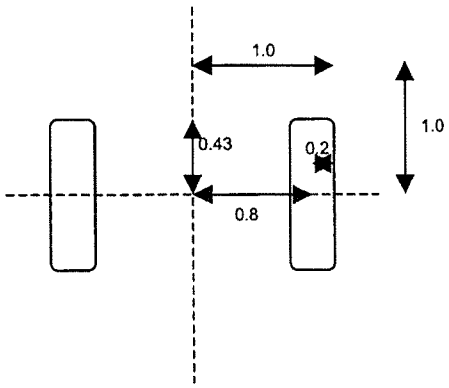

X-slot pole normalized dimensions

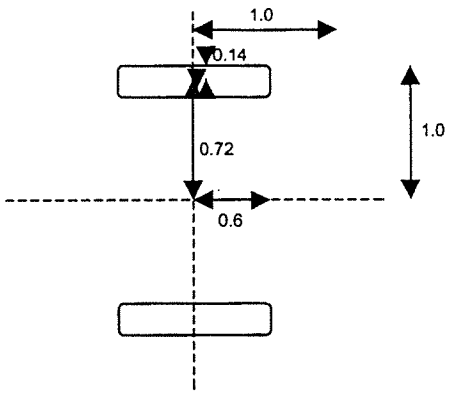

Y-slot pole normalized dimensions

Fig. 17. Normalized dimensions for each aperture

Next, the original condenser lens NA was determined under standard conditions by using Equation 2 and was found to be 0.26. Every dimension for both apertures was then multiplied by 0.26 to determine the new condenser lens numerical aperture. Finally, the new NAc's were divided by the objective lens NA (0.5) to determine each partial coherence value. The results are given in the following table.

	X-slot pole	Y-slot pole
NAc center	0.21	0.19
NAc radius	0.052	0.036
NAc z	0.11	0.16
σ center	0.42	0.38
σ radius	0.1	0.072
σ z	0.22	0.32

σ and NA results for both apertures

Fig. 18. This table shows the resulting partial coherence and numerical aperture values for both of the slot pole apertures.

Finally, the pitch ranges were calculated via Equations 8 and are shown here.

	Pmin (nm)	Pmax (nm)
X - Slot Pole	477	775
Y - Slot Pole	548	805

Range of Acceptable Pitches

Fig. 19. This table shows the range of pitches that should theoretically be printable with each aperture.

This means, for example, that for quarter micron line widths, the X-slot pole aperture should be able to print features with line to space duty ratios of approximately 1:1 to 1:2.

Next, wafers were coated and exposed using the previously determined conditions. Fortunately, this AMSL stepper measures intensity at the wafer and adjusts accordingly so that that exposure dose does not need to be changed. These wafers were exposed without any apertures as well as with both slot pole apertures using John Wintenzeller's Optical Proximity Correction mask (Mask name - JWOPC). Please see

Appendix A for operation procedures and Appendix C for instructions on inserting apertures. Once developed, the resulting resist images were examined via optical and scanning electron microscopes. An optical microscope was used first for a brief overview of each wafer and to ensure all exposed resist cleared during the develop process. Wafers were then looked at in both a Hitachi S-6780 CD SEM and a Philips 525 cross sectional SEM. The cross sectional SEM proved to be most useful in acquiring clear images of resist profiles but was unable to measure CD's. In order to use this SEM with resist images, wafers need to be cleaved into small (less than 2cm x 2cm) samples and sputtered in gold. Unfortunately, resist charging issues resulted in very little use of the Hitachi CD SEM, which was unable to accept the small, gold sputtered samples. Finally, the observed results were studied with respect to expectations which will be discussed shortly.

III. Results and Analysis

Since this project was mainly for education purposes, a great deal of time was spent ensuring that the material had been thoroughly understood. With that said, one of the most important results was actually seeing how the illumination at the wafer level changed as a result of off axis illumination. Figure 20 shows the resulting illumination with the x slot pole in place. We see this is quite different than the illumination profile under standard illumination seen back in Figure 2.

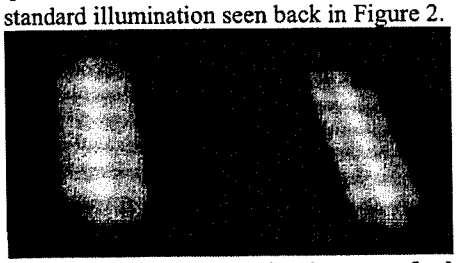

X-slot pole illumination at wafer level

Fig. 20. This is a picture taken with the x slot pole aperture in place on an ASML 5500/90 stepper. This image was achieved by opening the tool and moving the wafer stage out of the way.

Figure 21 provides an illumination of the features observed for the next few pictures.

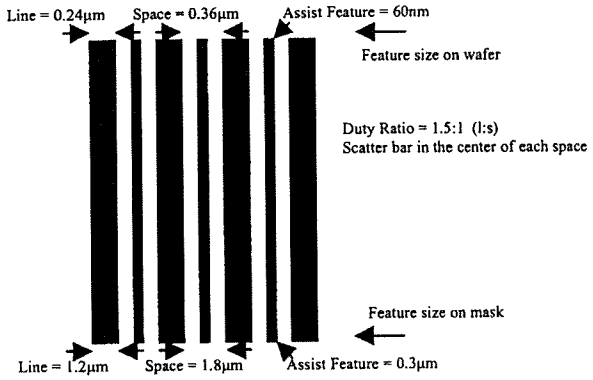

Feature design

Fig. 21. This is an illustration of one of the designs on the mask used for this project. Note that it contains OPC features which as will be seen were not able to resolve the 0.24um features under standard illumination conditions.

The next three pictures are from the Philips cross sectional SEM and were obtained by taking a digital camera picture of the monitor (at this time, this is the only way to capture images from this SEM).

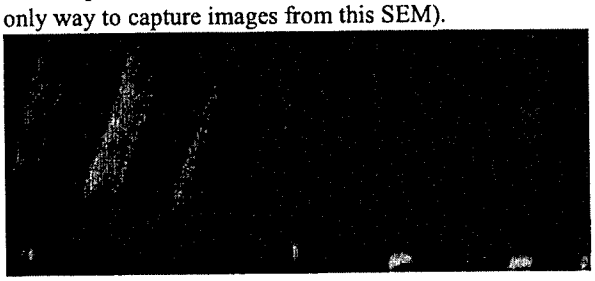

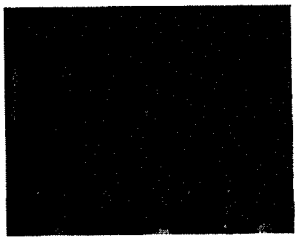

0.24μm lines

Fig. 22.

(a) X-slot pole
(b) Y-slot pole
(c) On axis illumination

These three images prove that off axis illumination in the form of slot poles functions as theoretically expected. First of all, Figure 22(c) shows that standard illumination is not able to resolve the 0.24μm features even with the help of the small OPC scatter bar feature. Figure 22(b) which was done with the y slot pole was also unable to resolve this feature size; this was also expected. Figure 22(a) on the other hand, shows the excellent results obtained with the x slot pole. In this case, 0.24μm features with a duty ratio of 1:1.5 were printed clearly and consistently with near vertical sidewalls. It also appears that, this aperture provided a very respectable usable depth of focus. There seemed to be very little image degradation through a focus range of almost 2μm.

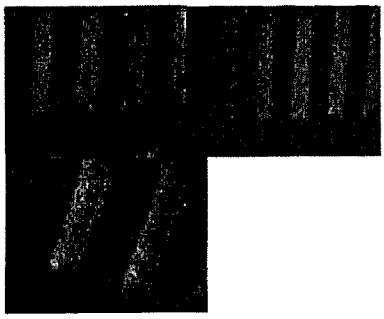

-1.0 -0.5 0.0

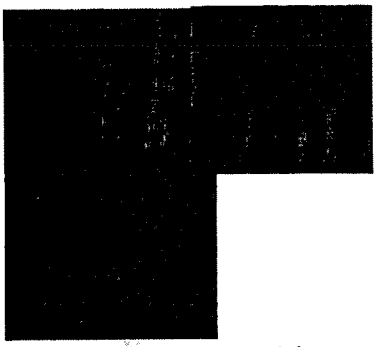

+0.5 +1.0 +1.5

Imaging as a function of focus offset

Fig. 23. The above pictures show how the image is affected by adjusting the focus offset.

It is clear from these images that the process quickly goes out of focus with positive levels of defocus. All of the tests performed indicate that although a zero focus offset may be optimal, there does not appear to be much of a loss in image quality for a large range of negative focus offsets on this tool.

A more surprising, if not totally unexpected result of this work was the imaging of what appear to be sub 0.20μm lines. One of the designs on the OPC mask looked as follows:

Feature design including sub 0.20μm scatter bar

Fig. 24. Illustration of design with sub 0.20μm scatter bar that was determined to print with off axis illumination.

It was previously determined that the x slot pole aperture was capable of printing features with pitches as large as 1:2. (Two spaces for every one line, or a 500nm space for every 250nm line). The above situation is clearly outside of this range for the main features, however, the scatter bars which fall exactly half way between each 0.24μm feature fall within the pitch limits. Also, with a feature size of around 200nm (for the scatter bars) they are still larger than the theoretical minimum of 124nm as calculated with Equation 3. We were surprised to find that these scatter bars resolved quite clearly as shown in the following images.

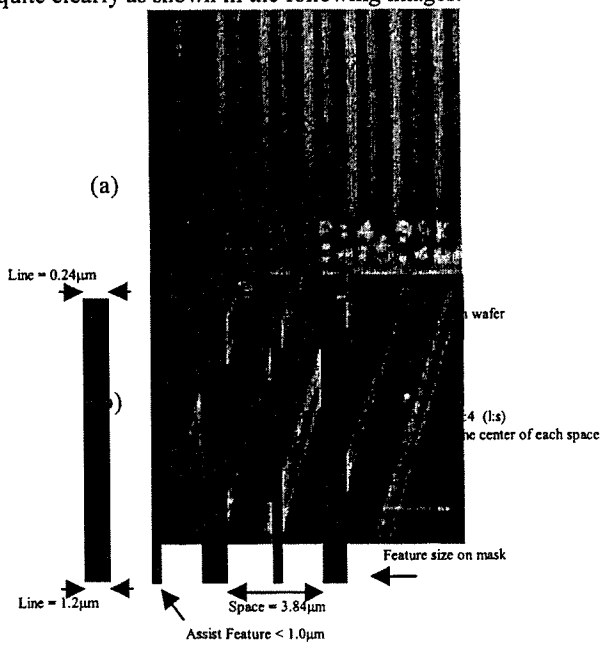

(c)

(d)

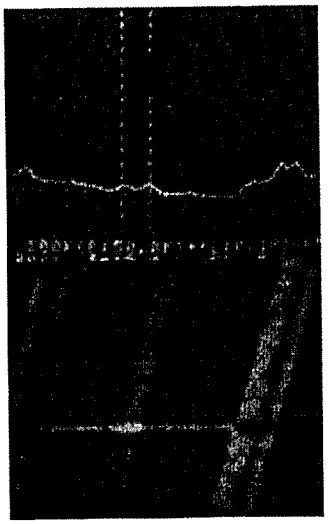

Sub 0.20μm features

Fig. 25. (a) and (c) are images taken on the Hitachi CD SEM and (b) and (d) are from the Philips cross sectional.

The four images above show that sub 0.20μm features can be printed on RIT's ASML DUV stepper with the aid of off axis illumination. Figure 25 (a) and (b) are images from the Hitachi CD SEM which are unfortunately very difficult to make out. The first image at a lower magnification shows that the scatter bars printed very consistently across the field. The third image labeled (c) was from an automatic CD measurement that measured one of these lines at 0.121μm as seen in the bottom right corner. It is doubtful that anything this small was printed and the measurement is most likely incorrect. Images from the Philips cross sectional SEM (b) and (d) provide clearer visuals of these lines and the highlighted section of the ruler on the screen indicates a distance of 1um. It is clear from image (d) that the scatter bar is smaller than $1/5^{th}$ of the 1μm section, therefore proving that it is thinner than 0.20μm. Unfortunately, at this time there are no metrology tools available at RIT to measure these features.

IV. Conclusions and Future Work

The effectiveness of off axis illumination has been successfully demonstrated as shown in this paper. Slot pole apertures based on dipole illumination theory were designed, fabricated, and implemented in an ASML 248nm DUV stepper system and were used to image quarter micron and smaller features.

There is a great deal of work to be done at RIT with this tool starting with the creation and optimization of standard processes with and without off axis illumination. Other illumination schemes including annular and quadrupole should be investigated. Also, it would be beneficial to determine the effectiveness of adding a pole centered at the origin to each one of these designs. If done correctly and carefully, the ASML 5500/90 could easily provide RIT with quarter micron capability.

Appendix A

Operating Procedures

ASML 5500/90 start up procedure from "power off" state

1. Ensure Chiller is on
    a. Breaker P7B2A #34-36-38 must be on and step up transformer must be on as well as card swipe ID.
2. Press "System On" (green button) in Electronics Control cabinet.
3. Press "Stepper On" (white button) in Electronics Control cabinet.
4. Go to the computer console
5. Type "n" and hit enter
6. Type "boot disk" (two words with a space)
    a. This will take several minutes
7. When asked to login, type "sys.6995" and press enter
    a. This will take several minutes
8. When asked to login to the PAS5500 Dialogue screen, type "msa" for login and press enter, then type "msa" for password and press enter
9. Once in the system you will follow the standard full start up procedures
10. Click "2 – Start-Up (Full)"
11. Click "Start"
    a. This will take about 10 mintues
    b. You should see the following warnings:
        i. "Wafer handling phase 5 not calibrated: No edge prealignment"
        ii. "No reference state defined for reflection image sensor"
        iii. Ignore any flow reading errors unless they equal 0

ASML Start Up from "power on" state

1. Exit to Main Menu if needed by selecting option "0 Exit"
2. Select option "1-Start-up/Shut-down"
3. Select option "2-Start-up(Full)"
4. Click "Start_"

    Note: This will take about ten minutes to warm up the tool and turn on all

subsystems. Once the system is ready it will go back to the Start-up(Full) screen.

5. Click "Exit"
    - Note: Tool will go into standby after a half an hour of nonuse.

****Bottom wafer in cassette is processed first**

Exposure Matrix (Full field exposure with no mask)

1. Exit to Main Menu if needed by selecting option "0 Exit"
2. Select option "6 Test Manager"
3. Select option "1 Run Test"
4. Click "Up..." to move to the top level of the directory
5. Click "Illumination System"
6. Click "Performance Tests"
7. Click "Resist Uniformity"
8. Click "Accept"
9. See attached page entitled **Exposure Matrix** for setup
10. Click "Accept"
    a. Automatically runs one wafer from input cassette once accepted.
    b. Optimum exposure is located at center of wafer.
    c. Pas5500 Graphics window will open automatically showing exposures
    d. Pas5500 Report window will open when wafer is done to show results. Report shows exposure pattern.

Focus/Exposure Matrix

1. Exit to Main Menu if needed by selecting option "0 Exit"
2. Select option "6 Test Manager"
3. Select option "1 Run Test"
4. Click "Up..." to move to the top level of the directory
5. Click "Projection System"
6. Click "FEM Developer/Customer"
7. Click "Accept"
8. See attached page entitled **Focus/Exposure Matrix** for setup
9. Click "Accept"

APPENDIX B

SETUP SCREENS FOR ASML TEST PROGRAMS

Exposure Matrix

```
Resist Uniformity Matrix

Nominal Energy   [mJ/cm2]   : __

Energy Increment [mJ/cm2]   : __

REMA Window Size [mm]  X : __    Y : __

Number of Dies         :    (Calculated automatically)

Load Reticle         : N_ []
```

FEM Screen

**Only modify highlighted fields. Acceptable values will be displayed at bottom of page when any field is selected.

```
Test Purpose          :Developer/Customer FEM

Expose Matrix Definition
  Matrix Size     Energy-x : __ Y-Focus : __
  Step Increment [um]    x : __ Y     : __
  Die A [mm]   Expose : __ []
  Die B [mm]   Expose : __ []
  Die C [mm]   Expose : __ []          X :
  Die D [mm]   Expose : __ []
  Die E [mm]   Expose : __ []
  Number of Dies to Expose     : __

Expose Conditions
  Focus [um]  Nominal : __ Step    : __
  Energy [mJ/cm2]  Nominal : __ Step    : __

  Reticle Handling    Load : __ []Unload  : __ []
  Reticle ID       :4357371N001
  Select

Reticle Pitches [mm]  1  : __          2 : __ 3 :__
Masking Window Size [mm]   X  : __     Y : __
Wafer Handling         Load : __ [] Unload : __ []

Waferscan and Die Flatness
  Max Number of Wafers    : __
  Scan Mode             : __
  Check Die Flatness          : __ []

Execute Zero Align        : __ []

Expose SEM Reference Marks     : __ []
Expose Energy to Clear Array      : __ []

Save Parameters    : __ []  Restore AMS-Defaults
```

APPENDIX C

INSTALLATION OF APERTURE BLADES

1. Obtain a small stepstool from line maintenance
2. Go to the side of the tool facing the hallways window.
3. Use the hook tool shown below to open the top panel of the tool located behind the reticle carrier.

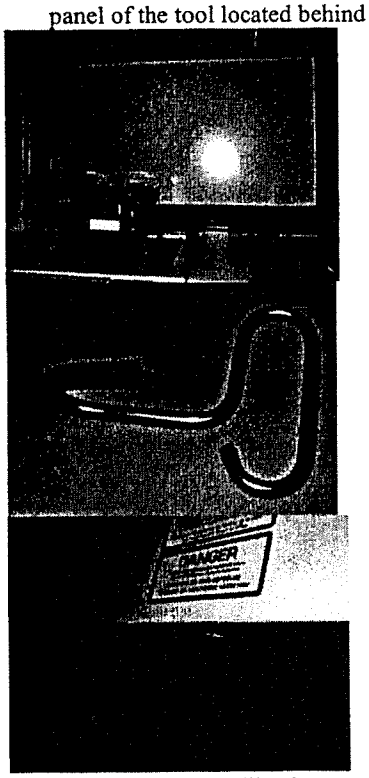

(Insert into the wholes like the one shown here)

4. Open the panel by pulling up with the hook in each hole (one at a time) until you feel it unlock.
5. Carefully remove the panel and set it against the wall.
6. Use a flat head screwdriver (with a large blade) to remove the four screws on the safety shutter. **Be careful not to strip the screws**

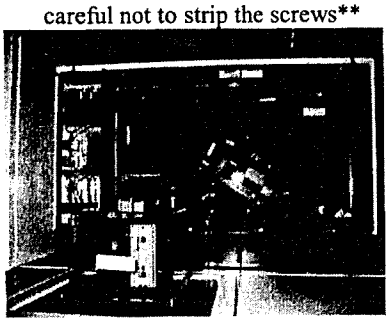

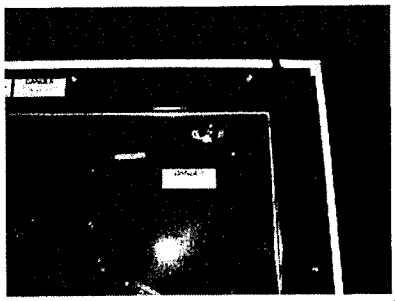

7. Carefully pull the UV shield out of the way.
8. Slide the desired aperture into the slot on the integrator lens element as shown. Be careful to observe the proper orientation

9. Put the UV shield back in place making sure that the small square piece of glass is in the bottom left hand corner. This is used to trigger the interlock switch.
10. Carefully screw all for screws back in place. They are spring loaded and only require ½ of a turn once seated properly.
11. Replace the outer cover and push firmly to ensure it is locked back in place.
12. Walk over to the laser house and push clear on the stand alone control panel.
13. Perform a fast start up as explained in the start up procedure.

a. If there is still an error regarding a shutter being open, or the laser is not turning on, push clear on the control panel by the laser once more and retry the fast startup. If it still doesn't work, contact John Nash and explain the situation.

APPENDIX D

USEFUL ASML 5500/90 SCHEMATICS FROM SYSTEM MANUAL

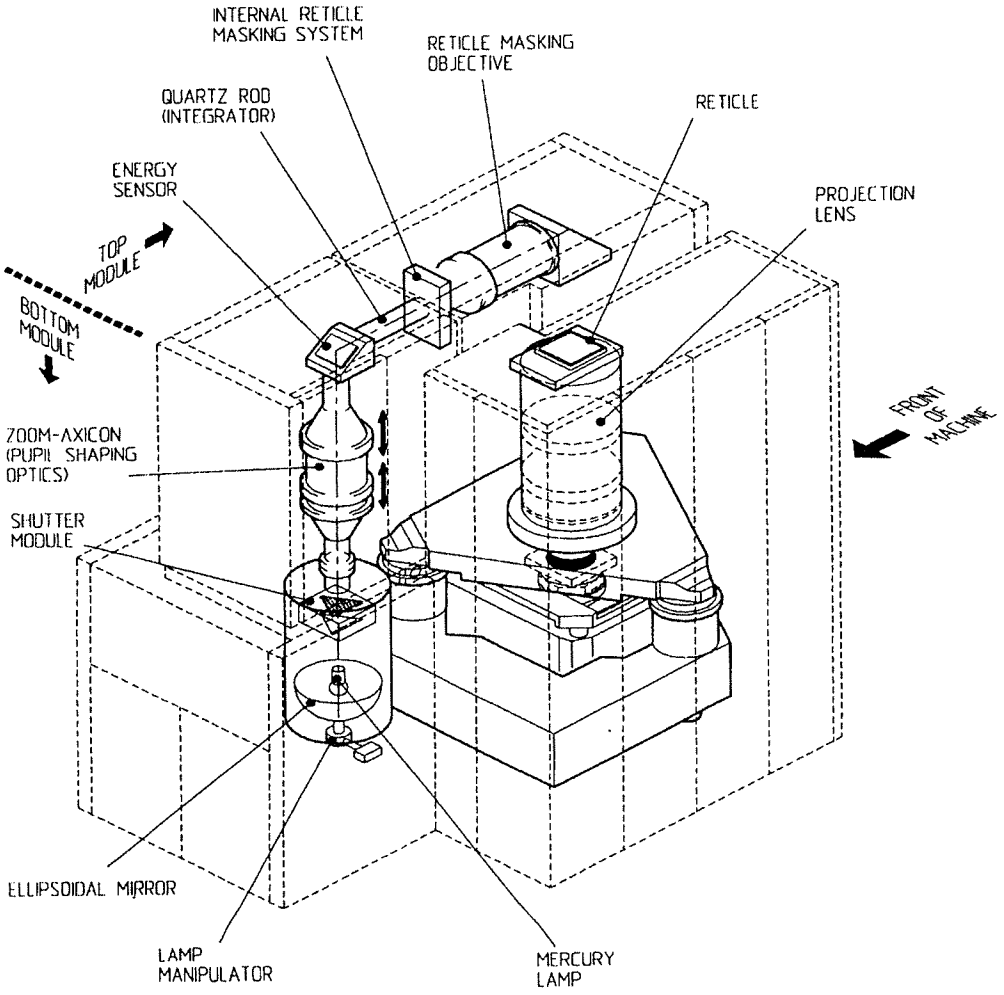

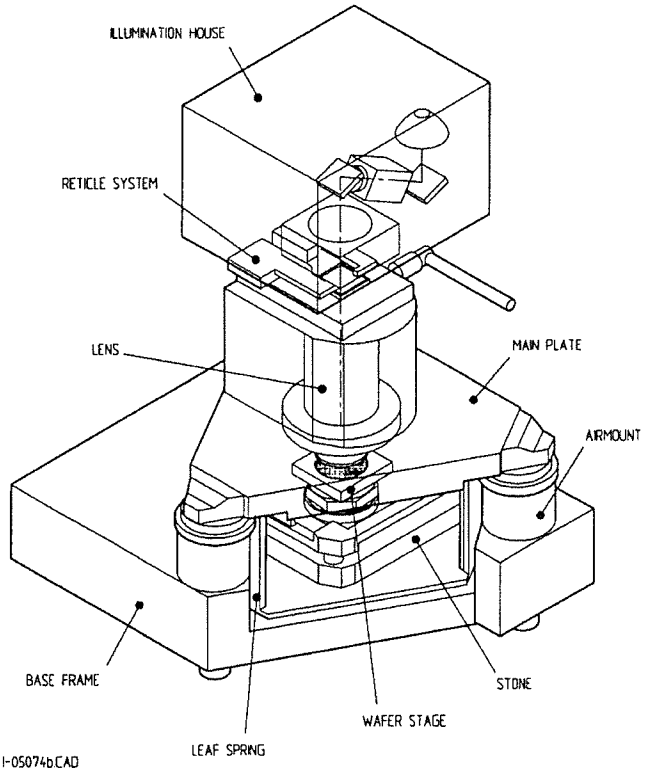

ACKNOWLEDGMENT

I am extremely grateful for all of the help and support I have received while working on this project. A special thanks goes to the following individuals: Dr. Bruce Smith for advising me in my work, professor Dale Ewbank for answering a million and one lithography questions, Microfab Technician John Nash for always being there to help out with the ASML stepper regardless of what time it was, Jay Cabacungan for staying in the cleanroom with me late into the night on several occasions and training me on a few key tools, Thomas Grimsley for teaching me how to use the cross sectional SEM and staying until 11:00pm to do so, Steven Kosciol and Dave Hathaway for their assistance in fabricating the apertures in the machine shop, John Wintenzeller for allowing me to use his project's photomask, Neal Lafferty for keeping the lab open late, and Nate Wescott for random assistance in the cleanroom.

REFERENCES

[1] C. A. Mack, "Depth of Focus," *Microlithography World*, Spring 1995, pp. 20, 1995.

[2] B. W. Smith, "Microlithography Science and Technology," Chapter 3, New York: Marcel Dekker, 1998, p.199.

[3] B. W. Smith, "Microlithography Science and Technology," Chapter 3, New York: Marcel Dekker, 1998, p.236.

[4] B. W. Smith, L. Zavyalova, J. S. Petersen, "*Illumination Pupil Filtering using modified quadrupole apertures*," Proc. SPIE Optical Microlithography XI, 1998, p.3334.

[5] K. Ronse and L. D. V. Hove, "*Resolution enhancement techniques in optical lithography*," IMEC. Semiconductor Fabtech, 10th Edition, p.242.

ASML System and Operation Manuals

Shipley DUVIII Data Sheets